



Geological environment problems during metro shield tunnelling in Shenzhen, China

Xi-Cun He¹ · Ye-Shuang Xu¹ · Shui-Long Shen² · An-Nan Zhou³

Received: 18 February 2019 / Accepted: 7 January 2020 / Published online: 16 January 2020
© Saudi Society for Geosciences 2020

Abstract

Shenzhen has abundant river systems, intense tectonic activity and complex geological conditions. The depth of Quaternary deposits is thin and uneven, and the primary bedrock comprises granite with various degrees of weathering, which covers more than 50% of the area of Shenzhen. Karst strata have developed in the eastern part of Shenzhen, and there are five groups of fracture zones in the area. Shenzhen also has some problematic soils, including granite residual soil, and muddy clay and silt. Metro tunnels are constructed using the shield tunnelling method. In Shenzhen, different strata are encountered during metro shield tunnelling, including upper-soft and lower-hard strata, hard rock strata, soft–hard alternating strata, under-crossing river or reservoir strata, muddy clay and silt strata and granite residual soil strata. The various strata encountered during shield tunnelling may result in a series of problems with the geological environment. Environmental geological problems during tunnelling are different for different strata, among which the major issues include serious cutter wear, difficulty in controlling the trajectory of the shield machine, shield machine jam, roof fall and slurry spewing. Different countermeasures should be implemented according to the characteristics of the strata to ensure the safe construction of metro tunnels. In this study, a case study of the Shenzhen Metro Line 10 is introduced, where tunnels pass through three specific strata: hard rock strata, boulder strata and under-crossing reservoir strata. In the future, more engineering cases that pass through different strata can be summarized according to the tunnel construction project in Shenzhen.

Keywords Geological formation · Geological environment problems · Metro tunnel · Shield tunnelling method · Shenzhen

Introduction

During the rapid economic development and urbanization in China over the last three decades, a large number of metro tunnels have been constructed (Xu et al. 2008; Shen et al. 2009, 2010; Qiao et al. 2017; Peng and Peng 2018; Wu et al. 2018a). Planning for urban rail transit in China began in the

1990s (Zhao et al. 2016; Lyu et al. 2018b), and there are currently 41 Chinese cities with metro tunnels either in operation or under construction, including Shanghai (Liao et al. 2009; Tan and Wang 2013a, 2013b; Shen et al. 2014; Lyu et al. 2019a, 2019b), Beijing (Liu et al. 2000; Chang 2013), Guangzhou (He et al. 2016; Ren et al. 2016; Lyu et al. 2016, 2018a), Jinan (Lyu et al. 2020), Hangzhou (Xu et al. 2017,

Responsible Editor: Rudrajit Mitra

✉ Ye-Shuang Xu
xuyeshuang@sjtu.edu.cn

✉ Shui-Long Shen
shensl@stu.edu.cn

Xi-Cun He
hexicun@sjtu.edu.cn

An-Nan Zhou
annan.zhou@rmit.edu.au

¹ State Key Laboratory of Ocean Engineering, Department of Civil Engineering, School of Naval Architecture, Ocean, and Civil Engineering, Shanghai Jiao Tong University, Shanghai 200240, China

² Department of Civil and Environmental Engineering, College of Engineering, Shantou University, and Key Laboratory of Intelligent Manufacturing Technology (Shantou University), Ministry of Education, Shantou 515063, Guangdong, China

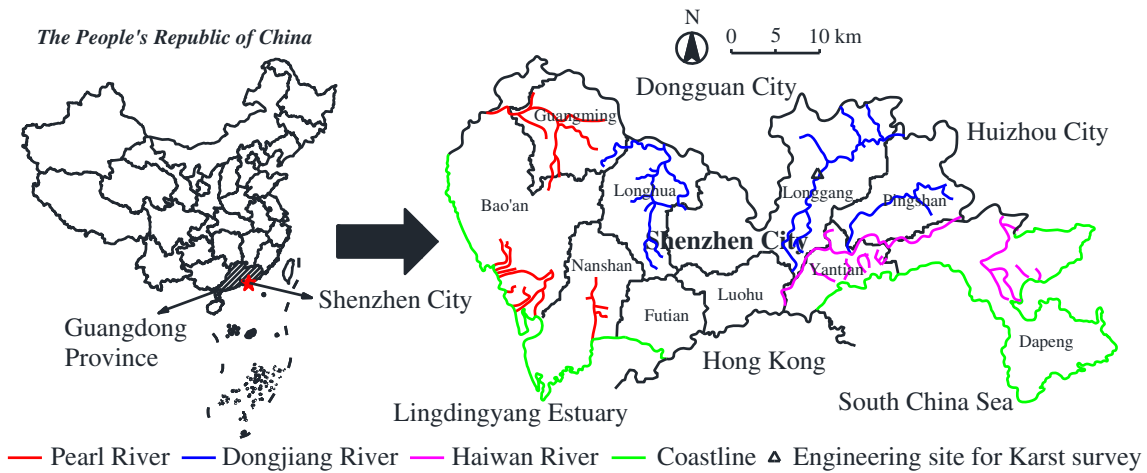
³ Civil and Infrastructure Engineering, School of Engineering, Royal Melbourne Institute of Technology (RMIT), Melbourne, Victoria 3001, Australia

2018a; Tan et al. 2018) and Shenzhen (Li and Chen 2012; Yang et al. 2016). For example, the metro system constructed in Shanghai has a track length of 666 km and consists of 16 lines and 389 stations (Xu et al. 2012, 2018b; Xu and Shen 2012; Wu et al. 2014, 2017b; SM 2018a). The metro system in Beijing has a track length of 597 km, consisting of 21 lines and 368 stations (Zhang et al. 2008; BS 2018). Shield tunnelling is the main construction method for metro tunnels. A series of problems related to the geological environment are encountered during the construction of metro tunnels (Ren et al. 2018a, 2018b). The geological characteristics vary in different cities, such as the soft soil in Shanghai (Xu et al. 2009, 2016; Elbaz et al. 2016), shallow biogas in Hangzhou (Xu et al. 2017, 2018) and water-rich strata in Tianjin (Shen et al. 2015; Wu et al. 2019). These geological environmental problems should be evaluated by considering the local geological characteristics.

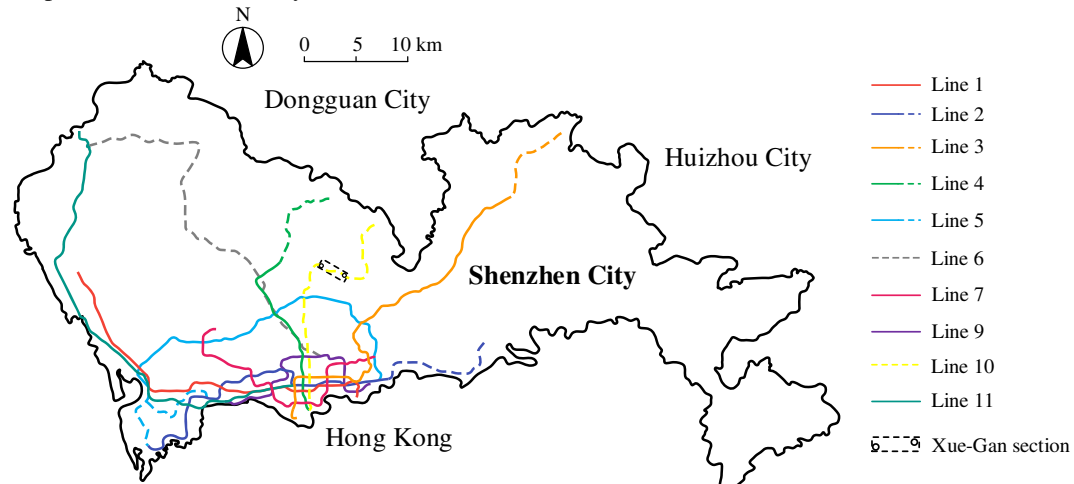
Shenzhen City in Guangdong Province is one of the most developed coastal cities in the south of China,

with an area of 1890 km². Figure 1 shows the administrative districts and layout of the metro system in Shenzhen. Shenzhen is located on the east side of the Pearl River Estuary and adjacent to the South China Sea, as shown in Fig. 1a. Construction of the metro system in Shenzhen began in 2004. Currently, the constructed metro in Shenzhen has a track length of 286 km and consists of eight lines and 199 stations (SM 2018b). The layout of the metro system, including the sections that are currently built and those under construction, is shown in Fig. 1b. Shenzhen has distributed reservoirs and abundant river systems, including the Dongjiang River, Haiwan River and Pearl River. The terrain of Shenzhen is high in the southeast and low in the northwest (LS 1983). Thus, the geological conditions in Shenzhen are complex and varied (SG 2009). The depth of the Quaternary deposits is thin and uneven. Granite with different degrees of

(a) Map of China and Shenzhen City



(b) Map of Shenzhen Metro system (built and under construction)



Note: solid lines indicate built metro lines and dash lines indicate under construction metro lines

Fig. 1 Map of administrative districts and metro system in Shenzhen (Based on Cui et al. 2016)

weathering is widely distributed as the primary bedrock and covers more than 50% of the area of Shenzhen, with an outcrop area of 760 km² (Zhang et al. 2014; Cui et al. 2016). This granite has a shallow buried depth, large thickness and significant spheroidal weathering (SG 2009). Karst strata have also developed in eastern Shenzhen. Furthermore, tectonic activity in the area is intense, and five large fault zones have developed in Shenzhen (SG 2009).

The typical buried depth of Shenzhen metro tunnels is 10–20 m below the surface, and the maximum depth is approximately 40 m (Li et al. 2014; Sun et al. 2015; SM 2018b). Given the complex geological conditions in Shenzhen, different strata are encountered during shield tunnelling, which can result in geological environmental problems. According to the urban plan for Shenzhen, more than 20 lines with a track length of 753 km will be in operation in the future (SM 2018b). To ensure the safe construction and operation of metro tunnels in Shenzhen, problems related to the geological environment should be considered in terms of the characteristics of the strata encountered during shield tunnelling. This will allow appropriate countermeasures to be adopted based on the characteristics of the strata and anticipated problems related to the geological environment.

The objective of this study is to investigate geological environmental problems during metro shield tunnelling in Shenzhen. First, the geological and hydrogeological characteristics of Shenzhen are introduced. Then, the geological environmental problems due to the strata encountered during shield tunnelling are investigated. Finally, appropriate countermeasures are proposed in consideration of a case study.

Geological and hydrogeological characteristics of Shenzhen

The landforms of Shenzhen can be divided into three types: mountain, terrace and coastal plain, which have elevations of 100–500, 10–80 and 0–10 m, respectively. Figure 2 shows the geology in Shenzhen. The bedrock of Shenzhen consists of different types of rocks, including sandstone, granite, mudstone, shale, limestone and marble. Granite is the primary bedrock and is widely distributed in Shenzhen. Quaternary deposits from 0 to 40 m are largely distributed in the western area of Shenzhen and occur sporadically in other areas (SG 2009). There is a large area of karst strata in eastern Shenzhen. Generally, the depth of metro tunnel construction is 10–40 m below the surface.

Quaternary deposits

Classification of quaternary deposits

Table 1 summarizes the detailed classification and characteristics of the Quaternary deposits in Shenzhen. The Quaternary deposits consist of the Holocene Series, upper Pleistocene Series and ungrouped residual layers. The sedimentary layer of the Holocene Series is relatively developed and consists of gravel, sand, sandy clay, clay, silt and peat, with a typical thickness of 10–20 m. The upper Pleistocene series is mainly composed of gravel, sand, sandy clay, silt and partially peat, with a typical thickness of 5–15 m. The ungrouped residual layers are mainly composed of gravel clay, sandy clay and cohesive soil, and the thickness is generally 0–64 m. Figure 3 shows a sectional view of the Quaternary deposits.

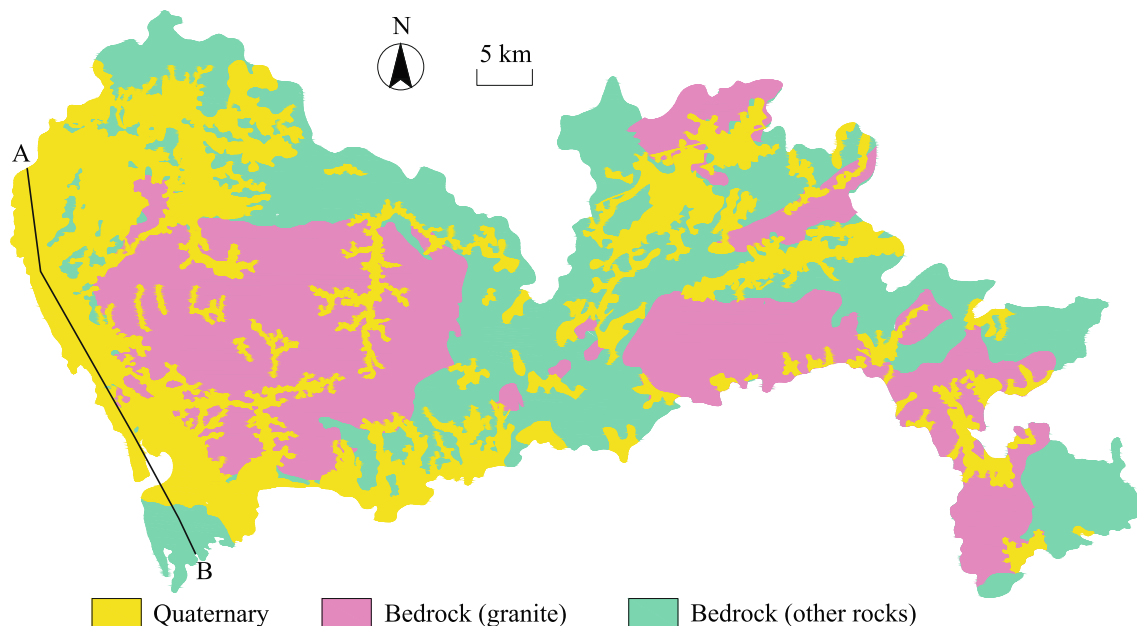


Fig. 2 Geology of Shenzhen (Based on SG 2009 and Cui et al. 2016)

Table 1 Detailed classification and characteristics of the Quaternary deposits (SG 2009)

Strata calendar	Geological strata		Characteristic	Distribution	Thickness (m)
	No.	Soil name			
Holocene series (Q _h)	Q _h ³ 1	Backfill	Clay and partial containing quartz breccia and weathered rock	–	2.2–4.9
	2 2–1	Silt	Grey-grey black; containing remains of marine life; saturated and incompact	River estuary, marine accumulation plains	4–22
	2–2	Silty fine sand	Grey-grey black, containing remains of marine life and rotten wood; saturated and incompact	Beach, marine accumulation plains	
	2–3	Muddy clay	Grey-dark grey; containing remains of marine life and rotten wood; saturated and incompact	Alluvial plain, marine accumulation plains	
	2–4	Coarse sand	Grey-dark grey; containing a small amount of organic matter; saturated; soft to flow plastic	Alluvial plain	
Q _h ² 3	3–1	Silty fine sand or muddy clay	Pale yellow or yellowish white; containing oyster shells and shellfish shards; saturated; incompact to slightly dense	Old sandbars, marine accumulation plains	5.1–6.9
	3–2	Coarse sand, gravelly sand	Grey-dark grey; partial containing rotten wood and shells; saturated; incompact to slightly dense	Alluvial plain, marine accumulation plains, lagoon plains	
	3–3	Clay, silty clay	Pale yellow; saturated and slightly dense	Alluvial plain, marine accumulation plains, lagoon plains	3.25–10
Q _h ¹ 4	4–1	Gravelly sand, pebble	Isabelline; containing a small amount of sand; wet; hard plastic to plastic	Alluvial plain	0–6.9
	4–2	Peaty clay	yellowish white to hoar; saturated; medium density-density	Alluvial plain	
Upper Pleistocene Series (Q _p)	Q _p ³ 5	Clay, silty clay	Dark grey; containing silt, fine sand and rotten wood; saturated; soft plastic to plastic	Platform recess, ancient gully	1.5–13.4
	Q _p ² 6	6–1 Medium sand, silty clay	Isabelline, yellowish white and fuchsia; containing a small amount of gravelly sand; wet; plastic to hard	Alluvial terrace	1.7–17.5
Q _p ¹ 7	6–2	Medium sand, coarse sand, gravelly sand	Greyish-hoar; containing pebble and clay	Alluvial terrace	
	7	Sand, silty clay	Maroon, iron red and yellowish white; containing lots of quartz and iron oxides; slight wet; hard plastic to hard	Upper part of the platform	1.5–8.4
Ungrouped residual layers (Q)	Q 8	Clay, sandy clay, gravelly clay	Pinkish red, isabelline and hoar; containing quartz breccia and boulder; soft plastic to plastic	Bedrock areas	0–64

Q_h³: Isotopic age (C¹⁴) is from 0.6 to 2.5 (ka B.P.); Q_h²: 2.9 to 4.9 (ka B.P.); Q_h¹: 5.1 to 8.8 (ka B.P.); Q_p³: 14.4 to 21.8 (ka B.P.); Q_p²: 22.7 to 30.4 (ka B.P.); Q_p¹: 32.6 to 38.5 (ka B.P.); Q: 100 to 700 (ka B.P.)

ka thousand years, B.P. before present

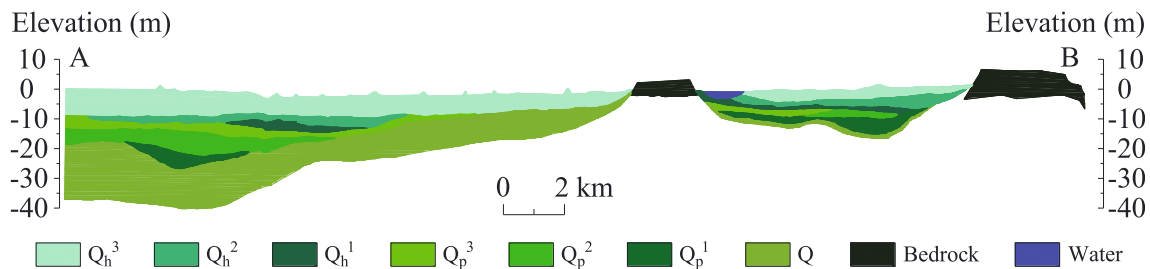


Fig. 3 Sectional view of the Quaternary deposits in Shenzhen (section A–B see Fig. 2)

Characteristics of quaternary soil

Figure 4 shows the typical physical and mechanical properties of the Quaternary soil in Shenzhen. Soil layer no. 2 mainly contains silt, silty fine sand, muddy clay and coarse sand and is characterized by a high natural water content, large void ratio, low bearing capacity and high compression coefficient. Soil layer no. 3 contains silty fine sand, muddy clay, coarse sand, gravelly sand and silt clay, with characteristics which are slightly better than those of layer no. 2. Soil layer no. 4 contains gravelly sand, pebbles and peaty clay and is characterized by a low natural water content, high bearing capacity and low compression coefficient. Soil layer no. 5 contains clay and silty clay and is characterized by a low compression coefficient and low vertical hydraulic conductivity. Soil layer no. 6 contains medium sand, silty clay, coarse sand and gravelly sand and is characterized by a low void ratio and high bearing capacity. Soil layer no. 7 contains sand and silty clay and is characterized by a high compression modulus and high bearing capacity. Soil layer no. 8 contains clay, sandy clay and gravelly clay and is characterized by high vertical hydraulic conductivity and high bearing capacity (SG 2009).

Muddy clay and silt soils

Muddy clay and silt are mainly distributed in the western coastal areas of the South China Sea and the eastern coastal areas of the Lingdingyang Estuary, covering an area of

approximately 60 km². The thickness of the silt is generally 3–10 m, with a maximum of over 20 m. Silt on the beach is mostly exposed to the surface and the water content in the upper part of these areas can be as high as 100% (essentially in a flowing state) with a self-stable slope of less than 5°. The muddy clay buried in the marine–continental alternating sedimentary facies in the sea alluvial plain has a water content of 40–60% and is in a state of flowing plasticity (SG 2009).

Weathered granite

Different weathering degrees

Based on the degree of weathering, the granite in Shenzhen can be divided into six types: residual soil, completely weathered granite, highly weathered granite, moderately weathered granite, slightly weathered granite and fresh rock. Table 2 summarizes the classification of granite weathering zones.

The thickness of granite weathering zones varies greatly, even within the same degree of weathering. Generally, the thickness of the highly weathered zone is approximately 10 m. However, in the southeast area of the Futian district, the thickness of the highly weathered zone reaches 30–40 m; in some areas, the thickness is greater than 80 m. The thickness of the moderately weathered zone also varies significantly, and it may be greater than 10 m and less than 1 m in some building sites.

Fig. 4 Typical physical and mechanical properties of Quaternary soil (Data from SG 2009)

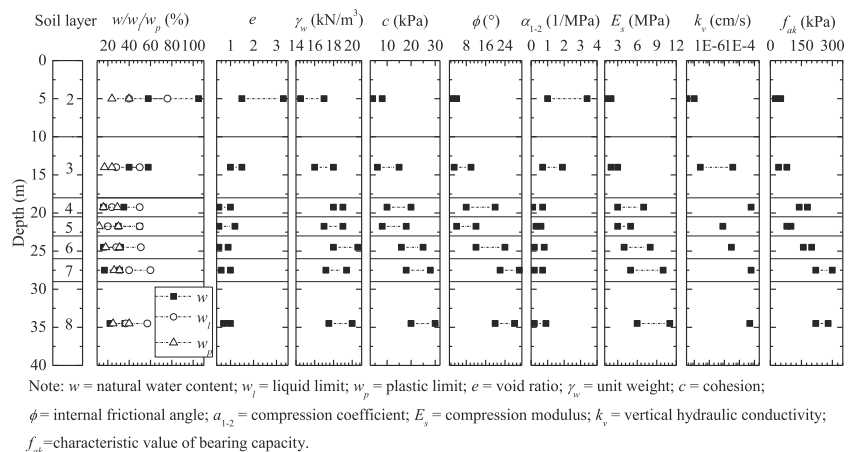


Table 2 Classification of granite weathering zone in Shenzhen (SG 2009)

Sequence (from top to bottom)	Name of weathered belt	Degree of decomposition
I	Residual soil	Complete
II	Completely weathered zone	Extremely high
III	Highly weathered zone	Extremely high to high
IV	Moderately weathered zone	High to moderate
V	Slightly weathered zone	Slight
VI	Fresh rock	Undecomposed

Residual soils

There are large areas of thick granite residual soils distributed in the Futian, Nanshan and Bao'an districts of Shenzhen, whereas the residual soils in the eastern part of Longgang are relatively thin (Dai et al. 2009). The water content of granite residual soil is high, and the porosity ratio is close to or greater than 1.0. The compression capacity is large, and the compression modulus is generally 4–6 MPa. The mineral composition of granite residual soil is primarily quartz, which accounts for approximately 60%; the remaining clay minerals are mainly kaolinite, with a lower content of illite. Most of the granite residual soils originated from coarse-grained granite and are gravel cohesive soils with a relatively limited water content, good permeability, small compressibility, fast consolidation and high bearing capacity; these can function as a good bearing layer for multi-storey buildings.

Spheroidal weathering

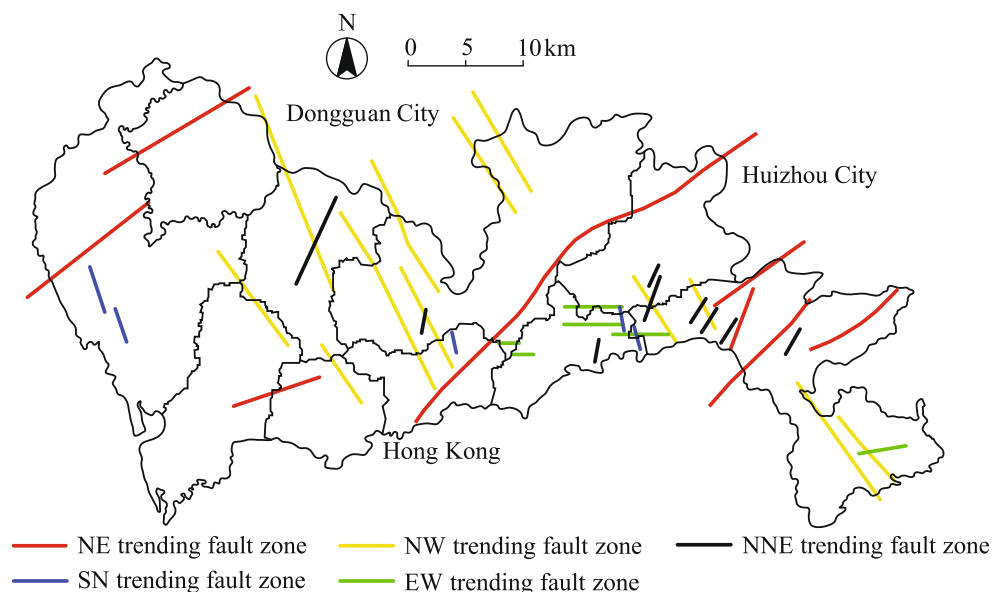
Joints in several directions divide the rock mass into polyhedral blocks. The edges and corners of these blocks are

weathered and destroyed by the effects of temperature and water in multiple directions and over a large depth range. Over a long period of time, the edges and corners of a rock block gradually disappear, and the block eventually transforms into an ellipsoidal or spherical shape. This phenomenon is called spheroidal weathering, which is a combination of dominant chemical weathering and physical weathering.

Spheroidal weathering is a common phenomenon in granite weathering layers and appears in the granite residual soils, completely weathered zone, highly weathered zone and at the ground surface. The diameter of these spheres varies from as large as 10 m to as small as 0.1 m. The stratum containing the spheroidal weathering zone is called the boulder stratum in Shenzhen.

Fracture structure

Figure 5 shows the main fault zones in Shenzhen. The zones are divided into five groups according to the fault tendency: northeast (NE), east–west (EW), northwest (NW), north–northeast (NNE) and south–north (SN) trending fault zones (SG 2009). Each fault zone is composed of several individual faults.

Fig. 5 Main fault zones in Shenzhen (Based on SG 2009)

NE trending fault zone

The NE trending fault zones are large in scale, with a direction of 50–70° from north; they mainly incline to the southeast and northwest with a dip angle of 40–80°. Single faults mostly have lengths greater than 5–10 km and widths greater than 10–20 m. The greatest width of an individual fault is greater than 70 m. The influence bandwidth ranges from tens of meters to 300 m and has good continuity. In some cases, the NE trending fault zones cross the NNE or NW trending fault zones. The faults are mainly characterized by compression and torsion.

EW trending fault zone

The EW trending fault zones occur in the direction of 80–100° from north and incline to the south with a dip angle of between 50° and 80°. These faults can extend for more than 30 km. The influence bandwidth ranges from 100 to 300 m to 1.0–2.5 km. Individual faults typically have a length of 1–8 km. The single fault with the largest scale is 15 km in length and 5–20 m in width. The faults are mainly characterized by compression with a small degree of torsion.

NW trending fault zone

The NW trending fault zones occur in the direction of 300–330° from north and incline to the northeast with a dip angle of 45–80°. These faults control the micro-geomorphology, such as the valleys, streams and springs in Shenzhen. The length of the NW trending fault zones is 10–30 km, in which individual faults are typically 2–15 km in length and 2–30 m in width. The faults are characterized by multiple periods of tectonic movement, mainly by compression and torsion, with an anticlockwise twist.

NNE trending fault zone

The NNE trending fault zones occur in the direction of 20°–35° from north and incline to the northeast with a dip angle of between 40° and 80°. These faults are characterized by poor development, a small scale and sporadic a distribution. Most of the individual faults are straight and short. The early faults

are tensile, and the later faults are characterized by compression and torsion, with an anticlockwise twist.

SN trending fault zone

The SN trending fault zones occur in the direction of 345°–360° from north and mainly incline to the east with a dip angle of between 50° and 70°. These faults are characterized by poor development, a small scale and a sporadic distribution. The faults are mainly characterized by compression with a small degree of torsion.

Karst strata

Karst is primarily distributed in the eastern part of Shenzhen, particularly in the Longgang district. Based on the buried depth, karst can be classified as covered karst (with a buried depth of 4–40 m) and buried karst (with a buried depth of greater than 40 m). Based on the influence depth range of a general building load on the foundation and the probability of a surface karst collapse disaster (Lyu et al. 2017), covered karst is further divided into shallow buried areas (less than 15 m), intermediate buried areas (15–30 m) and deep buried areas (30–40 m). Buried karst is developed in glutenite and carbonate rocks. Table 3 summarizes the characteristics of karst caves in one engineering site, the location of which is shown in Fig. 1a. The rate of occurrence of holes with karst caves is between 41.8 and 78.8%.

Hydrogeological conditions

The groundwater in Shenzhen includes pore water, bedrock fissure water and karst water (SG 2009), as shown in Fig. 6. The groundwater level fluctuates between 2 and 3 m below the surface.

Pore water

Pore water is primarily distributed in the southwestern edge of Shenzhen. The aquifer layers have a sporadic and dispersed distribution and are mostly composed of fine sand, coarse sand and gravel layers. Water abundance is not uniform and varies from poor to moderate. The pore

Table 3 Statistics of karst caves in an engineering site (SG 2009)

Survey type	Overburden thickness (m)	<i>N</i>	<i>Nk</i>	<i>Nk/N</i> (%)	karst caves height (m)	Top elevation of karst caves (m)	Bottom elevation of karst caves (m)
Detailed survey	15.6–32.0	134	56	41.8	0.2–20.2	17.65–16.60	–22.83–14.59
Supplementary survey	17.39–40.74	66	52	78.8	0.1–15.0	–18.0–16.0	–18.25–21.90

N number of drilled holes, *Nk* number of drilled holes with karst caves

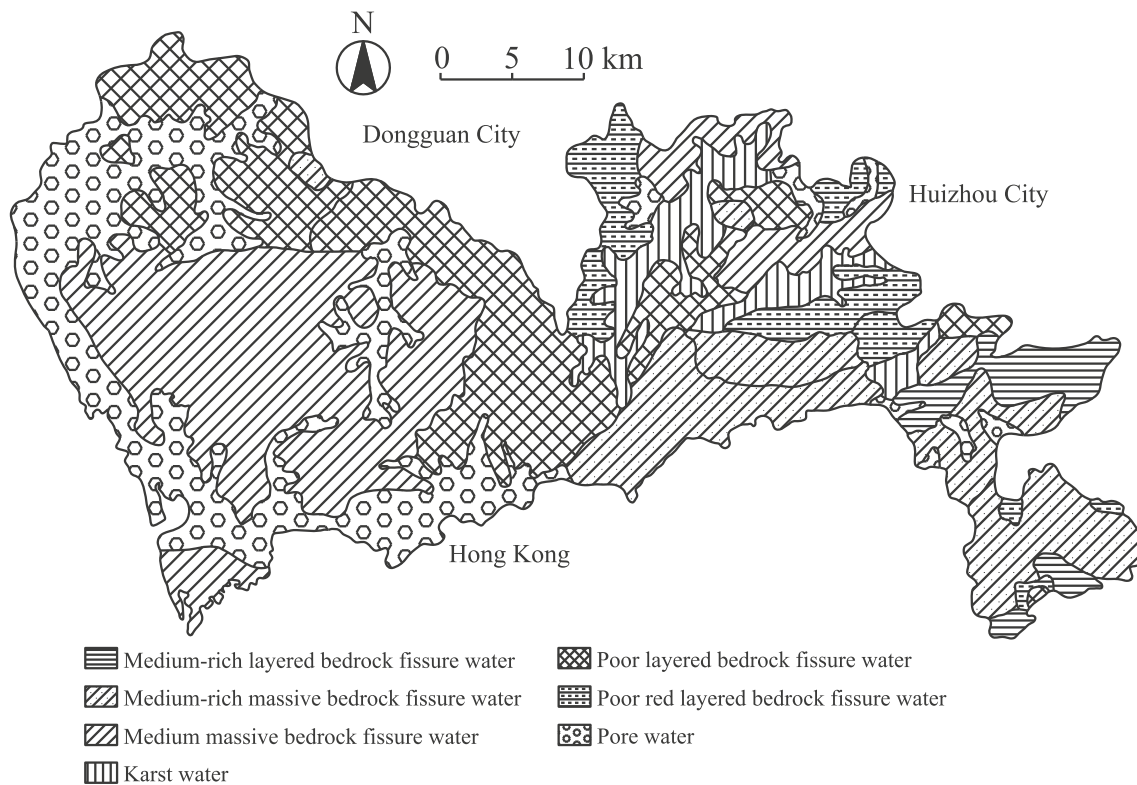


Fig. 6 Schematic of groundwater type distribution in Shenzhen (Based on SG 2009)

water in Shenzhen is divided into alluvial marine deposit pore water, residual deposit pore water and alluvial diluvium pore water. The water inflow of the alluvial marine deposit is poor, owing to the small interstices between the sand particles. The water inflow of a single well in the residual deposit is normally less than $100 \text{ m}^3/\text{day}$, whereas that of the alluvial diluvium deposit is abundant, with a maximum value of $1300 \text{ m}^3/\text{day}$.

Bedrock fissure water

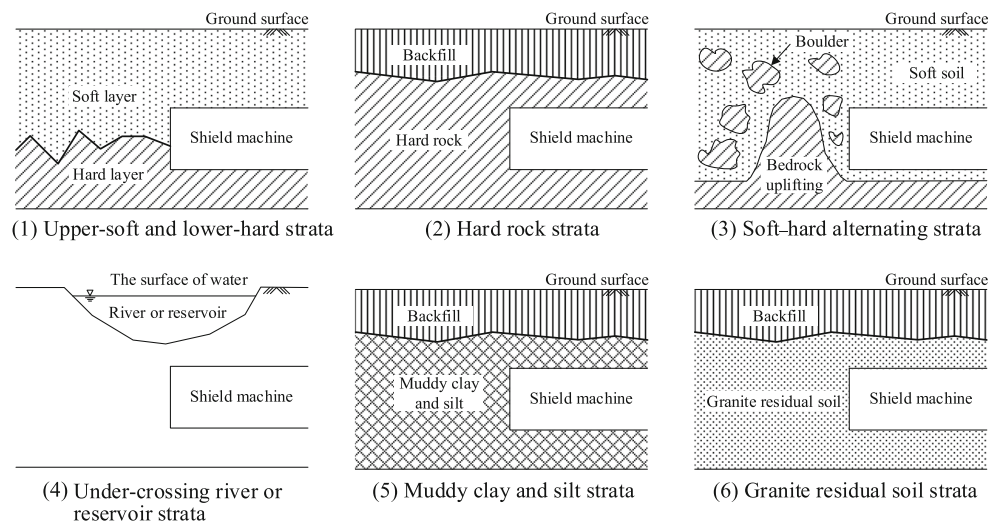
Fissure water is mainly distributed in mountainous and hilly areas. Bedrock fissure water is subdivided into layered bedrock fissure water, massive bedrock fissure water and red layered fissure water, based on the genetic type of the bedrock. Layered bedrock fissure water is mainly distributed in the central and northwestern regions of Shenzhen, with some in the eastern region. Massive bedrock fissure water is mainly distributed in the west and south of Shenzhen and covers 48.7% of the area of Shenzhen. The water abundance is poor or moderate, depending on the degree of fissure development in the layered or massive bedrock. The distribution range of red layered fissure water is limited and the water abundance is poor.

Karst water

Karst water is distributed in the karst basin located in the northeastern part of Shenzhen and is present in the karst fissures of dolomite, dolomitic limestone, dolomitic marble, marble, crystalline limestone and breccia limestone. The water abundance of karst aquifers is generally high, but is heterogeneous with obvious anisotropy. Generally, the water abundance is high in areas with strong karst development and less abundant karst caves, whereas the water abundance is poor in areas of converse characteristics.

Geological environmental problems during tunnel construction

Considering the geological and hydrogeological characteristics of Shenzhen, as shown in Fig. 7, the following strata may be encountered during shield tunnelling of metro tunnels, which may result in the occurrence of various geological environmental problems: upper-soft and lower-hard strata, hard rock strata (partially containing karst or faults), soft-hard alternating strata (including boulder strata and bedrock uplift strata), under-crossing river or reservoir strata, muddy clay and silt strata and granite residual soil strata.

Fig. 7 Schematic of shield tunnelling strata in Shenzhen

Upper-soft and lower-hard strata

An upper-soft and lower-hard stratum indicates that the excavation face encounters mixed ground containing a soft layer (e.g., clay) at the top and a hard layer (e.g., granite) at the bottom (Ren et al. 2016). Owing to the variable and uneven geological conditions and relatively thin Quaternary deposits in Shenzhen, metro tunnels are often dug in strata with lithological changes, particularly upper-soft and lower-hard strata (Liu 2010). The upper part of a typical upper-soft and lower-hard stratum is a gravel cohesive soil or completely weathered granite. These soils can be easily softened, disintegrated and weakened. The lower part is mostly composed of moderately weathered and slightly weathered granite, which have high compression strength.

When shield tunnelling is carried out in upper-soft and lower-hard strata, the uneven compression strength results in increased cutter wear (Elbaz et al. 2018a). Because the upper-soft stratum can easily enter the cutter chamber, whereas the lower-hard rock does not break easily, the trajectory of the shield machine is difficult to control. The resulting deviation in the tunnelling direction leads to additional frictional resistance, which reduces the tunnelling speed. If the parameters of the shield machine, such as the speed of the cutter head, torque of the cutter head and thrust of the oil cylinder, are not controlled effectively, slurry can be spewed (Peng 2015; Ren et al. 2016).

During the shield tunnelling construction of a certain interval of Line 2 of the Shenzhen Metro, the tunnelling parameters of the shield machine were abnormal, and the cutter wear was severe. A supplementary survey showed that there was a typical upper-soft lower-hard stratum approximately 50 m in length on the excavation surface, which consisted of an upper part of completely weathered granite and lower part of moderately and slightly weathered granite, with a uniaxial compressive strength of 137 MPa (Deng and Gu 2012).

Hard rock strata

Hard rock strata are particularly common in shield tunnelling in Shenzhen. In addition to uniform hard rock, shield machines also need to tunnel in hard rock strata with faults or karst in some cases. Typical hard rock strata have high quartz content and high brittleness. The compressive strength of hard rock strata is high, with a maximum uniaxial compressive strength of 295 MPa (Liu 2010). During the shield tunnelling construction of a certain interval of Line 5 of the Shenzhen Metro, a long-distance hard rock stratum was encountered, which accounted for 46.5% of the interval length. This hard rock stratum had a uniaxial compressive strength of greater than 100 MPa, and mainly consisted of granite, with a high quartz content, high brittleness and hard rock (Li et al. 2009). Because of the high compression strength of hard rock, the cutter wears easily. When the cutter is breaking hard rock, the rock exerts an anti-torque on the shield machine, which causes the shield machine to rotate by itself. Thus, the trajectory of the shield machine can be difficult to control. Segment stagger, segment damage and over-excavation can occur owing to deviations in tunnelling direction. In addition, segment stagger and damage can lead to segment leakage (Li et al. 2009). Changing the cutter frequently and correcting the trajectory of the shield machine reduces the overall tunnelling efficiency.

If there are faults in the hard rock, the rock is crushed and broken by the faults, thereby reducing rock stability. Once rock containing a fault is disturbed by the shield machine, ground settlement occurs (Hamid et al. 2015). Furthermore, the fractures in the fault zone can store a large amount of water, which can lead to slurry spewing (Ohbo et al. 2000; Liu et al. 2018; Zhang et al. 2018).

Moreover, karst action in soluble rocks results in the formation of karst caves in hard rock strata. Before a shield construction, the state of the karst caves is geologically stable. The surrounding fissures, the properties of the overlying soil layer

and the hydrodynamic conditions are almost unchanged in general. With the advance of the shield machine, the disturbance by the construction of the surrounding environment changes the surrounding fissures, the properties of the overlying soil layer and the hydrodynamic conditions, which in turn damage the constructed tunnels and shield machine (Cui et al. 2015). If some water is present in the karst caves, screw conveyor spewing can occur. More seriously, a large quantity of water can flow into the shield machine from the front of cutterhead, which would damage the shield machine and constructed tunnels. In addition, karst caves lead to long-term instability of the tunnel structure (Cui et al. 2015; Elbaz et al. 2018b).

Soft–hard alternating strata

Strata in front of the shield machine that comprise soft soil at first and then hard rock are called soft–hard alternating strata. Strata containing spheroidal weathering of granite are called boulder strata, which are a type of soft–hard alternating strata. The uniaxial compressive strength of a boulder can reach 200 MPa (Zhu et al. 2011). A stratum mainly consisting of soft soil with some bedrock uplifting is called a bedrock uplift stratum, which is another type of soft–hard alternating stratum. Boulders and bedrock are mainly distributed in the full weathering and strong weathering zones and sometimes appear in artificial backfill (Li 2017).

When a shield machine tunnels from soft soil to hard rock, the uneven strata cause the cutter to wear both rapidly and eccentrically (Ren et al. 2018c, 2018d). Because the boulder or bedrock cannot be thoroughly identified, the shield machine can easily become jammed and the tunnelling trajectory is difficult to control. Thus, the excavation face can easily be over-excavated, which would result in ground settlement (Liu 2010; Yang and Yuan 2011).

Under-crossing river or reservoir strata

Metro tunnels are often tunnelled under rivers or reservoirs in Shenzhen, as Shenzhen has abundant river systems. Because the depth of the Quaternary deposits in Shenzhen is thin, the overlying strata of the tunnels under crossing rivers or reservoirs are generally very shallow. The shield tunnel on a certain interval of Line 10 of the Shenzhen Metro passes under a reservoir three times. It is a shallow-covered tunnel with a minimum net distance of 4.36 m between the top of the shield tunnel and the bottom of the reservoir. Because of the small net distance between the top of the tunnel and the bottom of the river or reservoir, roof fall can readily occur in the tunnel. It is difficult to construct a self-supporting system in highly weathered strata after a construction disturbance, which can lead to cracking failure.

Muddy clay and silt strata

Most of the strata near the coastline in Shenzhen are muddy clay and silt strata, which are problematic soils with a low bearing capacity, high water content and highly thixotropy and rheology. Some metro tunnels along the coast have been tunnelled in a muddy clay and silt stratum, such as Line 5 of the Shenzhen Metro (Li 2017). The shield machine causes a large disturbance of this stratum during tunnelling, leading to deformation and instability (Shen et al. 2016; Wu et al. 2017a). Mud cake can easily form in the centre area of the cutter head, which results in decreased driving speed and increased cutting torque. At the same time, the increased temperature of the cutter chamber affects the service life of the main bearing seal. During the soil conveyor process, soil plugs are difficult to form because of the poor discharge capacity of the soil. As a result, soil spewing can easily occur at the position of the soil outlet. The stability of the excavation surface is poor, owing to the strong rheological properties of the muddy clay, and soil collapse can occur (Wu et al. 2018).

Granite residual soil strata

Granite residual soil is a problematic type of soil that differs from common cohesive soil. It is uneven, anisotropic and prone to softening, easy disintegration and disturbance. In the first phase of the Shenzhen Metro project, including construction of Line No. 1 in the East–West direction and Line No. 4 in the South–North direction, approximately 19 km of granite residual soils occur along the 24.4 km length of the entire line. In the granite residual soils, gravel clay accounts for 80–85%, sandy clay for approximately 15% and clay for less than 3% (Bao 2004). The strength of granite residual soil decreases with increasing water content, which renders the soil in front of the cutter head prone to collapse. Owing to the uneven weathering degree of granite residual soil, the strength of the granite residual soil varies, which makes the trajectory of the shield machine difficult to control. Because the granite residual soil is easily softened, the spewing phenomenon is severe, and the amount of slurry is large. If the shield machine deflects or the slurry spews, it is time-consuming to correct the direction of the shield machine or clean the slurry, which reduces the overall tunnelling efficiency.

Countermeasures for shield tunnelling in different strata

When shield tunnelling in different strata, appropriate countermeasures should be adopted to address the various problems related to the geological environment. Table 4 summarizes the main countermeasures for different strata. The countermeasures are described in detail in the references listed in

Table 4 Main countermeasures for different strata

Strata		Main countermeasures	References
Upper-soft and lower-hard strata		Adjusting the tunnelling parameters during tunnelling	Liu (2010); Fu (2009); Deng and Gu (2012)
Hard rock strata	Uniform hard rock strata	Controlling tunnelling parameters	Jin (2007)
	Hard rock strata with faults	Investigating the degree of cutter wear and replacing the cutter if necessary, sometimes consolidating the fault strata	Ohbo et al. (2000)
Soft–hard alternating strata	Hard rock strata with karst	Treating the karst caves	Cui et al. (2015)
	bedrocks uplift strata Boulders strata	Removing the uplift bedrocks or boulders	Zhang et al. (2011); Zhu et al. (2011); Jin et al. (2018a, 2018b)
Under-crossing river or reservoir strata		Increasing the thickness of overlying strata on the tunnel or reinforcing the overlying strata	Zhang et al. (2004)
Special soil strata	Muddy clay and silt strata	Improving the strata by grouting	Wang (2009); Gao (2012); Mu (2012); Shen et al. (2013); Cheng et al. (2017, 2018)
	Granite residual soil strata		

Table 4. The main countermeasures for different strata are as follows:

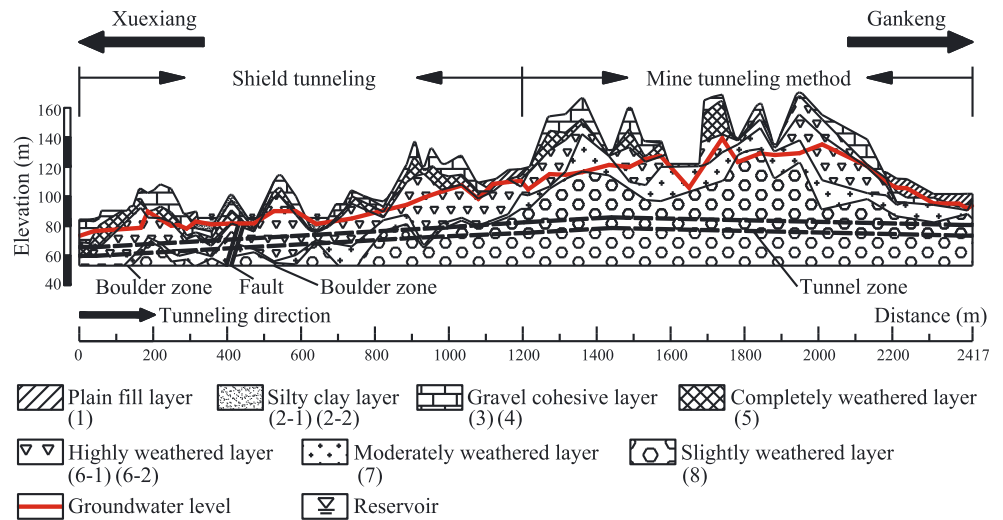
1. Upper-soft and lower-hard strata: the selection and layout of the cutters should focus on enhancing their adaptability to deal with the actual geological conditions. Adjustments of the cutter head speed, cutter head torque, pressure of the cutter chamber and thrust of the oil cylinder can be used to control the trajectory of the shield machine.
2. Hard rock strata: during shield tunnelling in uniform hard rock strata, the tunnelling parameters of the shield machine should follow a principle of ‘high speed, small torque and large thrust to improve the trajectory control of the shield machine. During shield tunnelling in hard rock strata containing faults, the degree of cutter wear should be investigated before the shield machine enters the fault zone. If the wear capacity of the cutter radius reaches 20–25 mm, the cutter should be replaced in advance to ensure that the shield machine can pass through the fault zone without stopping. In some cases, the fault strata should be consolidated through grouting. During shield tunnelling in hard rock strata with karst caves, all of the karst caves should be treated before tunnelling.
3. Soft–hard alternating strata: generally, the uplift bedrock and small boulders can be broken directly by the cutter of the shield machine. Large boulders should first be fractured into smaller rocks and then removed piece-by-piece by the shield machine.
4. Under-crossing river or reservoir strata: an economical method to increase the thickness of the overburden on the tunnel through filling of soils to the bottom of the river or reservoir is generally applied. Considering the requirements of shipping and drainage, grouting reinforcement of the bottom of the river or reservoir can be employed. Particularly in shallow overlying areas, grouting reinforcement and anti-floating structures should be simultaneously adopted.
5. Problematic soil strata: a horizontal twin-jet grouting method can be applied to control the shield posture as the shield machine begins tunnelling. During the shield tunnelling, strata grouting reinforcement methods can be used.

Case study

Project overview

The construction site is a tunnel section of the Xuexiang Station to Gankeng Station route (labelled as the Xue–Gan section) of Line 10 of the Shenzhen Metro; the interval length is 2417 m, as shown in Fig. 1b. The Xue–Gan section was constructed using shield tunnelling and mine tunnelling methods. Two earth pressure balance shield machines with

Fig. 8 Geological profile in Xue–Gan section of Line 10 of the Shenzhen Metro



diameters of 6 m were utilized. The lining of the tunnel has an outer diameter of 6 m and an inner diameter of 5.4 m.

Figure 8 shows the geological formation in the Xue–Gan section. Various strata have been identified: plain fill (labelled as 1), mucky cohesive soil (2–1), silty clay (2–2), pebbly clay (3), gravel cohesive soil (4), completely weathered granite (5), sandy highly weathered granite (6–1), massive highly weathered granite (6–2), moderately weathered granite (7) and slightly weathered granite (8). The physical and mechanical properties of the soil strata are given in Fig. 9. During shield tunnelling, the shield machine passed once through a hard rock stratum with faults, twice through boulder strata and three times through under-crossing reservoir strata. When the shield machine passes through the hard rock stratum with faults, ground settlement may occur. In the boulder strata, the cutter wears easily and the trajectory of the shield machine is difficult to control, which reduces the overall tunnelling efficiency. As for under-crossing reservoir strata, roof fall can occur in the tunnelling process. To ensure the shield machine passed through these strata efficiently and successfully, different countermeasures were adopted.

Hard rock strata with faults

The fault zone in the Xue–Gan section is not an active fault. It is located 412 m from Xuexiang station, is approximately 13 m in width and is part of the NW trending fault zone. Near the fault zone, the strata from top to bottom consist of completely weathered granite, highly weathered granite, moderately weathered granite and slightly weathered granite. The fault zone is developed and contains numerous cracks and broken rocks (e.g. mylonite, breccia), which have high water-permeability.

When the shield machine was 5 m from the fault zone, the wear capacity of the cutter wear radius was 23 mm. Therefore, the cutters with appropriate parameters were replaced to ensure the shield machine would pass through the fault zone without stopping. As the shield machine passed through the fault zone, synchronous grouting and secondary grouting were applied to control ground settlement. The average grouting quantity of the synchronous grouting was approximately 5 m³ per ring with a grouting pressure of 0.4 MPa, and that of the secondary grouting was approximately 8 m³ per

Fig. 9 Soil properties in Xue–Gan section of Line 10 of the Shenzhen Metro

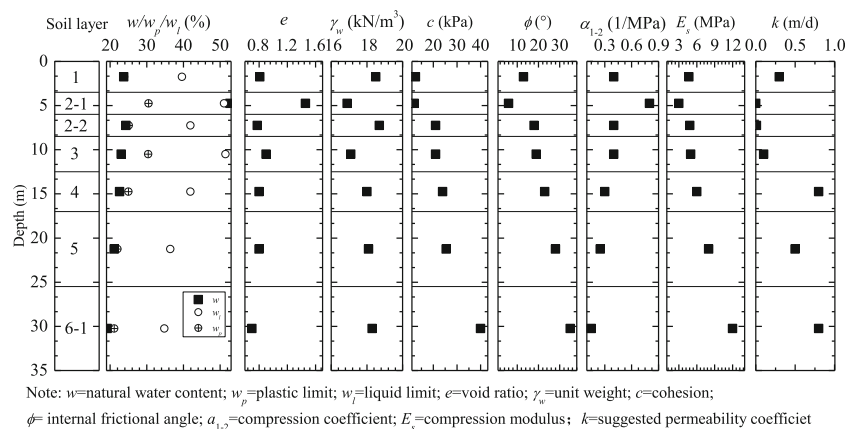


Table 5 Detailed information of the boulders

No.	Elevation (m)	Buried depth (m)	Thickness (m)	Degree of weathering
1	63.79–65.29	30.90–32.40	1.50	Massive high weathering
2	57.19–60.59	35.60–39.00	3.40	Massive high weathering
3	51.59–54.29	41.90–44.60	2.70	Massive high weathering
4	62.09–67.89	42.20–48.00	5.80	Moderate weathering

ring with a grouting pressure of 0.5 MPa. If the actual grouting quantity reaches the theoretical grouting quantity but the grouting pressure remains small, which indicates that the fault fractures are not completely filled, more grouting material should be injected. If the pressure increases sharply, which indicates that the gaps have been grouted tightly, grouting should be stopped immediately to avoid uplift of the ground surface with continued grouting.

Boulder strata

There are two boulder strata in the Xue–Gan section, located 130 and 526 m from Xuexiang Station. Four boulders were explored, and their detailed information is summarized in Table 5. These boulders are distributed 30–50 m below the ground surface in highly weathered strata. One boulder exhibits moderate weathering, and the others have massive high weathering with a thickness of 1.5–5.8 m.

The borehole blasting method was used to break up the boulders in this case. Figure 10 a shows a plan view of the blasting holes and monitoring holes in the ground surface above the boulder zones. For each boulder, two monitoring holes should be established to confirm the blasting quality. The blasting holes were drilled within the boulder boundary, and the horizontal spacing was 0.8 m. The diameters of the blasting and monitoring holes are both 110 mm. Figure 10 b shows a sectional view of the blasting holes. After drilling the holes to the bottom of the boulder, their quality should be checked. The permissible errors for the hole depth and hole spacing are both ±0.2 m, and that of the inclination is 2%. Explosives are placed in the holes to conduct the blasting. Finally, the blasting quality should be checked via the monitoring holes, and the diameter of the broken rocks should be controlled within 0.3 m.

Under-crossing reservoir strata

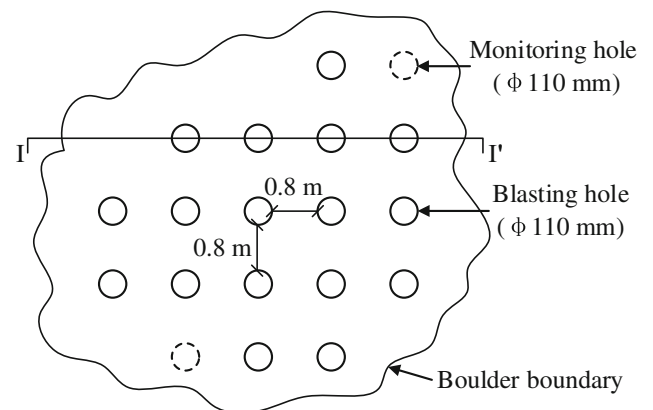
The shield tunnel passed under a reservoir three times, at locations 322, 472 and 602 m from Xuexiang station. The net distances between the top of the tunnel and the bottom of the reservoir are 10.028, 12.228 and 4.360 m, respectively. When the net distance between the top of the tunnel and the bottom of the river or reservoir is less than the minimum thickness of the overburden on the tunnel, the tunnel is defined as a

shallow-covered tunnel. Generally, the minimum thickness of the overburden on the tunnel (H) is determined according to the following equations (Zhang et al. 2004):

$$H = \frac{4F_t - 2c\sqrt{K_p} - H_w\gamma_w}{\gamma_w + (\gamma - \gamma_w)K_p} - \frac{D}{2} \tag{1}$$

$$K_p = \tan^2\left(45^\circ + \frac{\varphi}{2}\right) \tag{2}$$

(a) Layout of blasting holes and monitoring holes



(b) Sectional view along I-I'

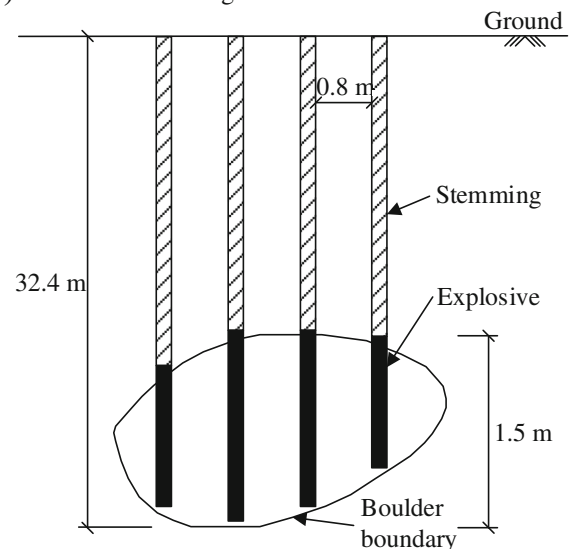


Fig. 10 Schematic of borehole blasting (Boulder No. 1 in Table 5)

where F_t is the thrust of the shield machine (kN), K_p is the coefficient of passive earth pressure, H_w is the depth of water (m), γ_w is the unit weight of water (kN/m^3), γ is the unit weight of soil (kN/m^3), c is the soil cohesion (kPa), φ is the internal friction angle of the soil ($^\circ$), and D is the tunnel diameter (m).

According to Eqs. (1) and (2), the minimum thickness of the overburden on the tunnel (H) is 6.445 m. Thus, the third

under-crossing is a shallow-covered tunnel with a net distance of 4.360 m, in which the strata mainly consist of highly weathered granite and silty clay with a loose structure that can be easily disturbed. The location relationship between the tunnel and Tuokeng reservoir is shown in Fig. 11a.

To ensure that the shield machine can pass through the under-crossing reservoir strata successfully, two measures are adopted during construction: (1) sleeve

Fig. 11 Shield tunnelling under-crossing the reservoir strata

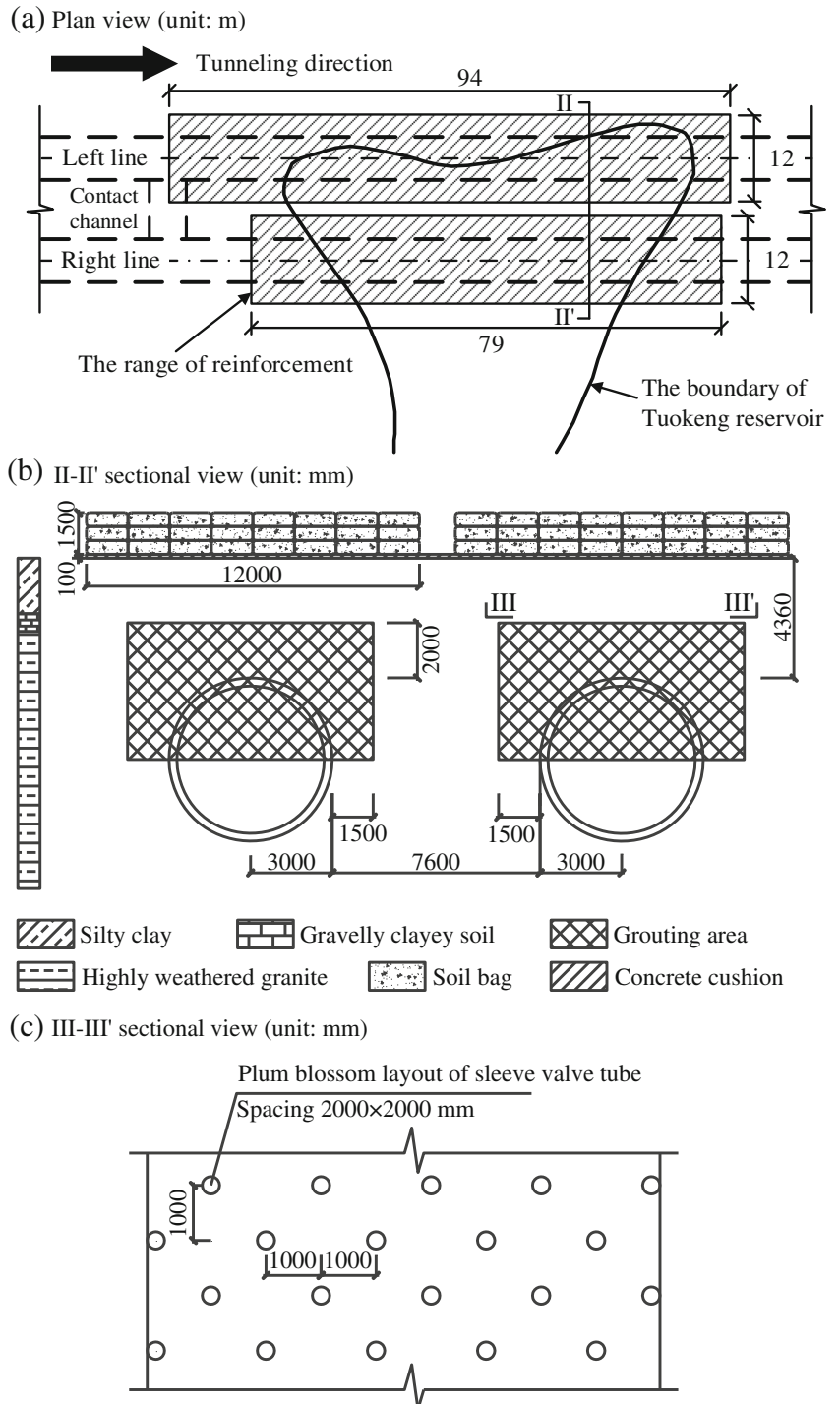
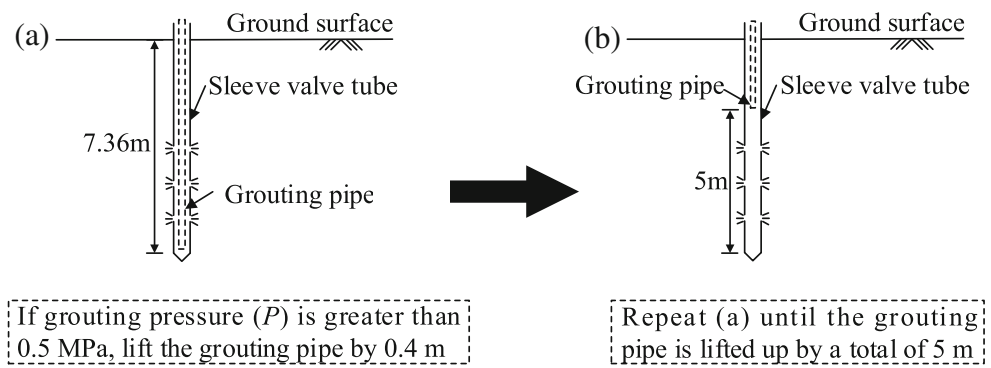


Fig. 12 Grouting process for one sleeve valve tube



valve tube grouting reinforcement and (2) preloading reinforcement at the bottom of the reservoir.

Sleeve valve tube grouting reinforcement

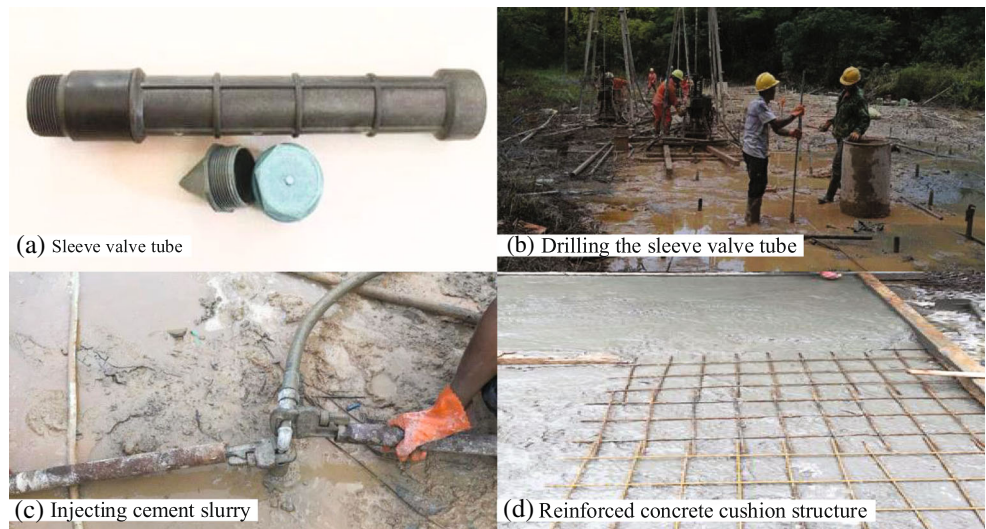
As shown in Fig. 11a, b, the width of the grouting reinforcement is 1.5 m beyond each side of the tunnel in the horizontal direction, the height is from the centreline of the tunnel to 2 m above the dome of the tunnel, and the length is 94 m for the left lane and 79 m for the right lane along the tunnelling direction. The spacing of the sleeve valve tube is 2×2 m with a triangular pattern, as shown in Fig. 11c. The inner diameter of the drilling hole is 56 mm, as shown in Fig. 13a. After drilling the hole, a sleeve valve tube with a total length of 11 m is inserted to a depth of 10 m (Figs. 12 and 13b). Then, ordinary Portland cement is injected to the bottom of the sleeve valve tube through a grouting pipe (Figs. 12 and 13c). The initial grouting pressure (P) is 0.2–0.5 MPa, and the grouting rate is 7–10 L/min. When P exceeds 0.5 MPa, the grouting pipe is raised through a distance of 0.4 m and the

grouting is continued (Fig. 12a). This process is repeated until the grouting pipe has been lifted through a total of 5 m (Fig. 12b). The grouting procedure should be repeated until all of the sleeve valve tubes are grouted, and the reinforcement range is completely filled.

Preloading reinforcement in the bottom of the reservoir

As shown in Fig. 11a, b, the width of preloading reinforcement is 6 m from the centreline of the tunnel, the height is 1.5 m, and the length is 94 m for the left lane and 79 m for the right lane along the tunnelling direction. After the sleeve valve tube grouting reinforcement is completed, $\text{Ø}8@150 \text{ mm} \times 150 \text{ mm}$ steel mesh is laid in the preloading reinforcement area and C20 concrete is then poured to a thickness of 100 mm to form a reinforced concrete cushion structure, as shown in Fig. 13d. After the structure reaches the desired strength, the soil bag is packed to preload the bottom of the reservoir.

Fig. 13 Site construction photographs of reinforcement for under-crossing reservoir strata in Xue-Gan section



Conclusions

The following conclusions can be drawn from this study:

1. The geological conditions of Shenzhen are complex and location-dependent. The Quaternary deposits are widely distributed in the western area of Shenzhen, with a shallow depth and uneven distribution. Granite is the primary bedrock in Shenzhen, and it has different degrees of weathering. Shenzhen has also developed problematic soils, including granite residual soil and muddy clay and silt. There are five developed fault zones. Karst is mainly distributed in the eastern area of Shenzhen. The groundwater in Shenzhen includes pore water, bedrock fissure water and karst water.
2. Owing to the complex geological conditions, during metro shield tunnelling, six specific strata may be encountered: upper-soft and lower-hard strata, hard rock strata (partially containing karst or faults), soft-hard alternating strata (including boulder strata and bedrock uplift strata), under-crossing river or reservoir strata, muddy clay and silt strata and granite residual soil strata. Considering the characteristics of these six types of strata, different problems related to the geological environment may arise, such as serious cutter wear, difficulty in controlling the trajectory of the shield machine, shield machine jam, segment stagger, segment damage, over-excavation, roof fall and slurry spewing.
3. To ensure the safety of tunnel construction, appropriate countermeasures should be adopted, such as adjusting the tunnelling parameters, consolidating the fault strata, treating the karst caves, removing the uplift bedrocks or boulders, increasing the thickness of overlying strata on the tunnel, reinforcing the overlying strata and improving the strata by grouting.
4. During construction of the Xue–Gan section of Shenzhen Metro Line 10, tunnels passed through hard rock strata with faults, boulder strata and under-crossing reservoir strata. Countermeasures such as the replacement of cutters in advance, synchronous grouting and secondary grouting were adopted for the hard rock strata with faults. A borehole blasting method was employed for the boulder strata. Grouting reinforcement and preloading reinforcement at the bottom of the reservoir were used for the under-crossing reservoir strata.

Funding information The research work described herein was funded by the Research Funding of the National Nature Science Foundation of China (NSFC) (Grant No. 41672259), Shantou University for New

Faculty Member (Grant No. NTF19024-2019) and Guizhou Science and Technology Project (Grant No. [2017]5402 & [2017]2814).

References

- Bao XD (2004) Engineering geological properties of the remainder soil from weathering granite in Shenzhen District. *Railw Investig Surv* 30(2):72–74 (in Chinese)
- Chang Z (2013) Public–private partnerships in China: a case of the Beijing no. 4 metro line. *Transp Policy* 30:153–160
- Cheng WC, Ni JC, Shen SL (2017) Experimental and analytical modeling of shield segment under cyclic loading. *Int J Geomech* 17(6): 04016146. [https://doi.org/10.1061/\(ASCE\)GM.1943-5622.0000810](https://doi.org/10.1061/(ASCE)GM.1943-5622.0000810)
- Cheng WC, Ni JC, Arulrajah A, Huang HW (2018) A simple approach for characterising tunnel bore conditions based upon pipe-jacking data. *Tunn Undergr Space Technol* 71:494–504
- Cui QL, Wu HN, Shen SL, Xu YS (2016) Geological difficulties and countermeasures for socket diaphragm walls in weathered granite in Shenzhen, China. *Bull Eng Geol Environ* 75(1):263–273
- Cui QL, Wu HN, Shen SL, Xu YS, Ye GL (2015) Chinese karst geology and measures to prevent geohazards during shield tunnelling in karst region with caves. *Nat Hazards* 77(1):129–152
- Beijing Subway (BS). (2018) Beijing subway operation corporate. Corporate official Website. <https://www.bjsubway.com/en/>
- Dai J, Gao GY, Wang TH (2009) Regional differences of granitic residual soil and research on its engineering characteristics. *Port Eng Technol* 46(1):56–59 (in Chinese)
- Deng B, Gu XF (2012) Shield construction technology in upper-soft lower-hard strata. *Mod Tunn Technol* 49(2):59–64 (in Chinese)
- Elbaz K, Shen JS, Arulrajah A, Horpibulsuk S (2016) Geohazards induced by anthropic activities of geoconstruction: a review of recent failure cases. *Arab J Geosci* 9(18):708
- Elbaz K, Shen SL, Cheng WC, Arulrajah A (2018a) Cutter-disc consumption during earth pressure balance tunnelling in mixed strata. *Geotech Eng ICE Proceedings* 171(4):363–376
- Elbaz K, Shen SL, Tan Y, Cheng WC (2018b) Investigation into performance of deep excavation in sand covered karst: a case report. *Soils and Foundations*, JGS 58(4):1042–1058. <https://doi.org/10.1016/j.sandf.2018.03.012>
- Fu YB (2009) Construction techniques by shield tunneling method in upper-soft lower-hard ground. *Technol Econ Areas Commun* 11(4):80–81 (in Chinese)
- Gao K (2012) Tunneling in mud/sand bursting geology by single-shield TBM. *Tunnel Constrution* 32(1):94–98 (in Chinese)
- Hamid C, Yilmaz O, Bahtiyar U (2015) Investigation of ground surface settlement in twin tunnels driven with EPBM in urban area. *Arab J Geosci* 8(9):7655–7666
- He L, Liang Q, Fang S (2016) Challenges and innovative solutions in urban rail transit network operations and management: China's Guangzhou metro experience. *Urban Rail Transit* 2(1):33–45
- Jin SH (2007) Countermeasures for earth pressure balance shield tunneling in hard rock section of Guangzhou metro. *Urban Rapid Rail Transit* 20(3):64–66 (in Chinese)
- Jin YF, Yin ZY, Wu ZX, Zhou WH (2018a) Identifying parameters of easily crushable sand and application to offshore pile driving. *Ocean Eng* 154:416–429
- Jin YF, Yin ZY, Wu ZX, Daouadji A (2018b) Numerical modeling of pile penetration in silica sands considering the effect of grain breakage. *Finite Elem Anal Des* 144:15–29
- Landform of Shenzhen (LS) (1983) Science and technology press. People's Republic of China, Guangdong (in Chinese)
- Li J (2017) Analysis of boulders and uplift tunnel construction techniques. *Chin Overseas Archit* 5:215–217 (in Chinese)

- Li JS, Chen HC, Li Z (2014) Key construction technologies for shield-bored tunnel of Chegongmiao Station-Hongshuwan Station section on no. 11 line of Shenzhen metro crossing closely above existing metro line. *Tunnel Constr* 34(4):374–379 (in Chinese)
- Li MW, Liu JG, Han XF, Chen SG (2009) Key technologies of long-distance shield boring in hard rock. *Tunn Constr* 29(4):470–474 (in Chinese)
- Li X, Chen X (2012) Using grouting of shield tunneling to reduce settlements of overlying tunnels: case study in Shenzhen metro construction. *J Constr Eng Manag* 138(4):574–584
- Liao SM, Liu JH, Wang RL, Li ZM (2009) Shield tunneling and environment protection in Shanghai soft ground. *Tunn Undergr Space Technol Inc Trenchless Technol Res* 24(4):454–465
- Liu JG (2010) Countermeasures for shield tunnelling in soft and hard uneven strata of Shenzhen metro. *Modern Tunn Technol* 47(5):17–21 (in Chinese)
- Liu W, Luo F, Mei J (2000) A new construction method for a metro station in Beijing. *Tunn Undergr Space Technol* 15(4):409–413
- Liu XX, Shen SL, Xu YS, Yin ZY (2018) Analytical approach for time-dependent groundwater inflow into shield tunnel face in confined aquifer. *Int J Numer Anal Methods Geomech* 42(4):655–673
- Lyu HM, Wang GF, Shen JS, Lu LH, Wang GQ (2016) Analysis and GIS mapping of flooding hazards on 10 May, 2016, Guangzhou, China. *Water* 8(10):447. <https://doi.org/10.3390/w8100447>
- Lyu HM, Wang GF, Cheng WC, Shen SL (2017) Tornado hazards on June 23rd in Jiangsu Province, China: preliminary investigation and analysis. *Nat Hazards* 85(1):597–604. <https://doi.org/10.1007/s11069-016-2588-2>
- Lyu HM, Sun WJ, Shen SL, Arulrajah A (2018a) Flood risk assessment in metro systems of mega-cities using a GIS-based modeling approach. *Sci Total Environ* 626:1012–1025. <https://doi.org/10.1016/j.scitotenv.2018.01.138>
- Lyu HM, Shen JS, Arulrajah A (2018b) Assessment of geohazards and preventative countermeasures using AHP incorporated with GIS in Lanzhou, China. *Sustainability* 10(2):304. <https://doi.org/10.3390/su10020304>
- Lyu HM, Shen SL, Zhou A, Yang J (2019a) Risk assessment of mega-city infrastructures related to land subsidence using improved trapezoidal FAHP. *Science of The Total Environment*:135310. <https://doi.org/10.1016/j.scitotenv.2019.135310>
- Lyu HM, Shen SL, Yang J, Yin ZY (2019b) Inundation analysis of metro systems with the storm water management model incorporated into a geographical information system: a case study in Shanghai. *Hydrology and Earth System Sciences* 23(10):4293–4307
- Lyu HM, Sun WJ, Shen SL, Zhou AN (2020) Risk Assessment Using a New Consulting Process in Fuzzy AHP. *Journal of Construction Engineering and Management* 146(3):04019112
- Mu YZ (2012) Analysis and countermeasures of settlement for shield tunnelling in sand cobble stratum. *Railway Constr Technol* 4:65–68 (in Chinese)
- Ohbo N, Furuya T, Takamatu K, Komaki S (2000) Seismic behavior of shield tunnel across active fault
- Peng J, Peng FL (2018) A GIS-based evaluation method of underground space resource for urban spatial planning: part 1 methodology. *Tunn Undergr Space Technol* 74:82–95
- Peng Y (2015) EPB shield tunneling through the bumps formation associated soft-hard bedrock construction measures. *Guangdong Archit Civil Eng* 1:59–62 (in Chinese)
- Qiao YK, Peng FL, Wang Y (2017) Monetary valuation of urban underground space: a critical issue for the decision-making of urban underground space development. *Land Use Policy* 69(12):12–24
- Ren DJ, Shen SL, Arulrajah A, Wu HN (2018a) Evaluation of ground loss ratio with moving trajectories induced in double-O-tube (DOT) tunnelling. *Can Geotech J* 55(6):894–902. <https://doi.org/10.1139/cgj-2017-0355>
- Ren DJ, Xu YS, Shen JS, Zhou AN (2018b) Prediction of ground deformation during pipe-jacking considering multiple factors. *Appl Sci* 8(7):1051. <https://doi.org/10.3390/app8071051>
- Ren DJ, Shen JS, Chai JC, Zhou AN (2018c) Analysis of disk cutter failure in shield tunnelling using 3D circular cutting theory. *Eng Fail Anal* 90(2018):23–35. <https://doi.org/10.1016/j.engfailanal.2018.02.015>
- Ren DJ, Shen SL, Arulrajah A, Cheng WC (2018d) Prediction model of TBM disc cutter wear during tunnelling in heterogeneous ground. *Rock Mech Rock Eng* 51(11):3599–3611. <https://doi.org/10.1007/s00603-018-1549-3>
- Ren DJ, Shen SL, Cheng WC, Zhang N, Wang ZF (2016) Geological formation and geo-hazards during subway construction in Guangzhou. *Environ Earth Sci* 75(11):934
- Sun B, Xiao LG, Jiang H, Sun ZY, Li ST (2015) Numerical simulation of mutual influence in construction of parallel overlapping tunnels of Shenzhen metro. *Tunnel Constr* 35(7):616–622 (in Chinese)
- Shanghai Metro (SM) (2018a) Shanghai Shentong metro group corporate. Corporate official Website. <http://service.shmetro.com/en/>
- Shenzhen Metro (SM) (2018b). Shenzhen metro group corporate. Corporate official Website. <http://www.szmco.net/page/eng/index.html/>
- Shen SL, Du YJ, Luo CY (2010) Evaluation of the effect of rolling correction of double-o-tunnel shields via one-side loading. *Revue Canadienne De Geotechnique* 47(10):1060–1070
- Shen SL, Horpibulsuk S, Liao SM, Peng FL (2009) Analysis of the behavior of DOT tunnel lining caused by rolling correction operation. *Tunn Undergr Space Technol* 24(1):84–90
- Shen SL, Wu HN, Cui YJ, Yin ZY (2014) Long-term settlement behaviour of metro tunnels in the soft deposits of Shanghai. *Tunn Undergr Space Technol Inc Trenchless Technol Res* 40(12):309–323
- Shen SL, Wang ZF, Yang J, Ho CE (2013) Generalized approach for prediction of jet grout column diameter. *J Geotech Geoenviron* 139:2060–2069
- Shen SL, Wu YX, Xu YS, Hino T, Wu HN (2015) Evaluation of hydraulic parameters from pumping tests of multi-aquifers with vertical leakage in Tianjin. *Comput Geotech* 68:196–207
- Shen SL, Cui QL, Ho CE, Xu YS (2016) Ground response to multiple parallel microtunneling operations in cemented silty clay and sand. *J Geotech Geoenviron* 142(5):04016001. [https://doi.org/10.1061/\(ASCE\)GT.1943-5606.0001441](https://doi.org/10.1061/(ASCE)GT.1943-5606.0001441)
- Shenzhen Geology (SG) (2009) Geology press, Beijing, People's Republic of China (in Chinese)
- Tan Y, Wang D (2013a) Characteristics of a large-scale deep foundation pit excavated by the Central-Island technique in Shanghai soft clay. II: top-down construction of the peripheral rectangular pit. *J Geotech Geoenviron Eng* 139(11):1894–1910
- Tan Y, Wang D (2013b) Characteristics of a large-scale deep foundation pit excavated by the Central-Island technique in Shanghai soft clay. I: bottom-up construction of the central cylindrical shaft. *J Geotech Geoenviron Eng* 139(11):1875–1893
- Tan Y, Jiang WZ, Luo WJ, Lu Y, Xu CJ (2018) Longitudinal sliding event during excavation of feng-qi station of Hangzhou metro line 1: Postfailure investigation. *J Perform Constr Facil* 32(4):04018039
- Wang L (2009) Mechanism and application of horizontal twin-jet grouting in soft ground. Dissertation, Shanghai Jiao Tong University (in Chinese)
- Wu HN, Huang RQ, Sun WJ, Shen SL, Xu YS, Liu YB, Du SJ (2014) Leaking behavior of shield tunnels under the Huangpu River of Shanghai with induced hazards. *Nat Hazards* 70(2):1115–1132
- Wu HN, Shen SL, Yang J (2017a) Identification of tunnel settlement caused by land subsidence in soft deposit of Shanghai. *J Perform Constr Facil* 31(6):04017092. [https://doi.org/10.1061/\(ASCE\)CF.1943-5509.0001082](https://doi.org/10.1061/(ASCE)CF.1943-5509.0001082)
- Wu HN, Shen SL, Yang J, Zhou AN (2018) Soil-tunnel interaction modelling for shield tunnels considering shearing dislocation in

- longitudinal joints. *Tunneling and Underground Space Technology* 78:168–177. <https://doi.org/10.1016/j.tust.2018.04.009>
- Wu YX, Lyu HM, Han J, Shen SL (2019) Case study: dewatering-induced building settlement around a deep excavation in the soft deposit of Tianjin, China. *J Geotech Geoenviron Eng, ASCE*, accepted, published on line
- Wu YX, Lyu HM, Shen JS, Arulrajah A (2018a) Geological and hydrogeological environment in Tianjin with potential geohazards and groundwater control during excavation. *Environ Earth Sci* 77: 392
- Wu YX, Shen JS, Cheng WC, Hino T (2017b) Semi-analytical solution to pumping test data with barrier, wellbore storage, and partial penetration effects. *Eng Geol* 226:44–51. <https://doi.org/10.1016/j.enggeo.2017.05.011>
- Xu YS, Shen SL (2012) Analysis of urbanisation-induced land subsidence in Shanghai. *Nat Hazards* 63(2):1255–1267
- Xu YS, Shen SL, Cai ZY, Zhou GY (2008) The state of land subsidence and prediction approaches due to groundwater withdrawal in China. *Nat Hazards* 45(1):123–135
- Xu YS, Shen SL, Du YJ (2009) Geological and hydrogeological environment in Shanghai with geohazards to construction and maintenance of infrastructures. *Eng Geol* 109(3–4):241–254
- Xu YS, Ma L, Shen SL, Sun WJ (2012) Evaluation of land subsidence by considering underground structures that penetrate the aquifers of Shanghai, China. *Hydrogeol J* 20(8):1623–1634. <https://doi.org/10.1007/s10040-012-0892-9>
- Xu YS, Wu HN, Shen JS, Zhang N (2017) Risk and impacts on the environment of free-phase biogas in quaternary deposits along the coastal region of Shanghai. *Ocean Eng* 137:129–137
- Xu YS, Shen JS, Zhou AN, Arulrajah A (2018a) Geological and hydrogeological environment with geohazards during underground construction in Hangzhou: a review. *Arab J Geosci* 11(18):544
- Xu YS, Shen SL, Lai Y, Zhou AN (2018b) Design of Sponge City: lessons learnt from an ancient drainage system in Ganzhou, China. *J Hydrol* 563(2018):900–908. <https://doi.org/10.1016/j.jhydrol.2018.06.075>
- Xu YS, Shen SL, Ren DJ, Wu HN (2016) Analysis of factors in land subsidence in Shanghai: a view based on strategic environmental assessment. *Sustainability* 8(6):573(1–12). <https://doi.org/10.3390/su8060573>
- Yang J, Chen J, Le X, Zhang Q (2016) Density-oriented versus development-oriented transit investment: decoding metro station location selection in Shenzhen. *Transp Policy* 51:93–102
- Yang XF, Yuan H (2011) The detecting and measure of the boulder layer at the site of Guangzhou metro line 3. *Constr Mechanization* 32(6): 73–76 (in Chinese)
- Zhang CX, Zheng TH, Yu ZJ (2014) The characteristics and influence to subway construction of weathered granite in Shenzhen area. *Railw Investig Surv* 5:26–29 (in Chinese)
- Zhang H, Chen SG, Tan XR, Zhao YB (2011) Study on boulder treatment in shield tunneling. *Constr Technol* 40(19):78–81 (in Chinese)
- Zhang Q, Han B, Li D (2008) Modeling and simulation of passenger alighting and boarding movement in Beijing metro stations. *Transp Res C* 16(5):635–649
- Zhang QH, Wang ST, Yan CZ, Zhang W (2004) Tunneling methods through river (lake, sea) bed under shallow covering by shield. *Chin J Rock Mech Eng* 23(5):857–857 (in Chinese)
- Zhang N, Shen JS, Zhou AN, Arulrajah A (2018) Tunneling induced geohazards in mylonite rock fault with rich groundwater: a case study in Guangzhou. *Tunn Undergr Space Technol* 74:262–272
- Zhao JW, Peng FL, Wang TQ, Zhang XY, Jiang BN (2016) Advances in master planning of urban underground space (UUS) in China. *Tunn Undergr Space Technol* 55:290–307
- Zhu WB, Huang WR, Meng QB, Hong Y (2011) Blasting technology for boulders and bedrock intrusions in shield engineering. *Modern Tunnelling Technology* 48(5):12–17 (in Chinese)